Decoupled genetic and epigenetic variation at local scale in an endemic and a widespread *Erodium* (Geraniaceae) species

Rubén Martín-Blázquez[1*], Mónica Medrano[1], Pilar Bazaga[1], Francisco Balao[2], Ovidiu Paun[3], Conchita Alonso[1*]

1. Estación Biológica de Doñana, CSIC, Avenida Américo Vespucio 26, Sevilla 41092, Spain.

2. Departamento de Biología Vegetal y Ecología, Universidad de Sevilla, Apdo. 1095, 41080 Sevilla, Spain.

3. Department of Botany and Biodiversity Research, University of Vienna, 1030 Vienna, Austria.

* Corresponding authors: rmartinblazquez@gmail.com and conalo@ebd.csic.es

Abstract

Epigenetic states offer an additional layer of variation besides genetic polymorphism that contribute to phenotypic variation and may arise either randomly or in response to environmental factors. We hypothesize that closely related species with different life-histories and habitat requirements could show distinct patterns of intraspecific epigenetic variation. We used Restriction-site Associated DNA sequencing (RADseq) and its bisulfite-converted variant (bsRADseq) to investigate in Sierra de Cazorla (SE Spain) the genetic and epigenetic population structure of two congeneric species, the endemic woody perennial *Erodium cazorlanum* and the widely distributed annual herb *E. cicutarium*. Population genomics analyses revealed no structure in either *E. cazorlanum* and *E. cicutarium,* suggesting substantial gene flow between the study populations. In contrast, we found that the mean proportion of global DNA methylation was different between populations and species, with *E. cazorlanum* DNA showing higher methylation average and across-individuals variation. For each species, we searched for the loci with the strongest epigenetic differentiation between populations (differentially methylated cytosines, DMCs), and summarized them across regions (differentially methylated regions, DMRs). Multivariate analysis and hierarchical clustering of single cytosines' methylation percentages did not group individuals by population, pointing to high epigenetic variation within populations. DMRs were enriched in *Copia* transposable elements, putatively associated with stress response in plants. Our results suggest that variation at both genetic and epigenetic levels in our study area occur mainly within natural populations of *E. cazorlanum* and *E. cicutarium,* with stronger population structure in *E. cicutarium,* and highlight the relevance of analyzing short distance spatial patterns.

Keywords: plant population epigenomics, bsRADseq, DNA methylation, epigenetic variation, cytosine differential methylation

37 **1. Introduction**

38 Understanding the sources of natural phenotypic variation is a crucial question in ecology and
39 evolution. The idea that epigenetic diversity can compensate for reduced genetic diversity,
40 promoting phenotypic variation through trait plasticity in response to environmental changes is
41 relatively new (Balao et al., 2018; Bossdorf et al. 2008; Richards et al., 2017; Richards, 2006;
42 Williams et al., 2023). Trait plasticity can be particularly advantageous for sessile organisms such
43 as plants, with limited escape strategies to face environmental perturbations and, thus, the
44 magnitude and population structure of genetic and epigenetic diversities in plant species with
45 disparate genomic and ecological features warrants comprehensive investigation (Anderson &
46 Gezon, 2015; Herrera et al.,2022; Richards et al., 2017; Szukala et al., 2023). Such knowledge
47 can help to optimize decisions in conservation (i.e. accurately evaluating the adaptive potential of
48 populations, Lamka et al., 2022; Williams et al., 2023), or even predict how plant species would
49 fare when introduced in foreign ecosystems (i.e., assess invasive potential, Hawes et al., 2018).

50 DNA methylation remains a focus of interest among the spectrum of plant epigenetic
51 modifications. The mechanistic control and effects of DNA methylation, its relationship with
52 other chromatin regulators such as histone tail modification and small RNAs, and the potential
53 transgenerational transmission of different methylation-marker types have been mainly studied in
54 model species such as *Arabidopsis thaliana* (Cokus et al., 2008; Muyle et al., 2022; Stroud et al.,
55 2014), and economically important species such as maize and rice (reviewed by Varotto et al.,
56 2022; but see also Herrera et al., 2018). Several DNA-methyltransferases set methyl groups in the
57 carbon-5' of cytosines followed by specific nucleotide motifs in the genome, referred to as
58 methylation contexts. In plants, there are three cytosine methylation contexts: CpG, CHG and
59 CHH (where H can be any nucleotide but G), which are each regulated by the action of distinct
60 enzyme complexes, and appear unevenly represented in plant genomes (Law & Jacobsen, 2010).
61 Symmetrical methylation in CpGs can be preferentially found in promoters and exons within
62 genes (referred to as gene body methylation; Bewick & Schmitz, 2017) and can be more
63 frequently heritable compared to other contexts (Schmitz et al., 2011). In turn, methylated CHGs

64 and CHHs are more abundant in heterochromatic and intergenic regions, and are often reset
65 between generations or rapidly (de)methylated in response to changes in environmental
66 conditions (Bouyer et al., 2017; Du et al., 2012). Furthermore, transposable elements (TEs) show
67 DNA methylation in all three contexts, resulting in TE silencing and promoting genome stability
68 (Matzke & Mosher, 2014). Given the wide range of genome sizes in plants, and the positive
69 relationship between genome size and TE proportion in the genome (Kidwell, 2002), plant species
70 show a broad variation in the level of DNA methylation, that was found to be related to
71 phylogenetic relationships and species genome size (Alonsoet al., 2019a; Alonso et al., 2015;
72 Vidalis et al., 2016).

73 The genomic and ecological features that could be associated to the broad variation in levels of
74 DNA methylation mentioned above are still poorly understood. Particularly for non-model plant
75 species, contrasting evidences have been found regarding their variation across natural
76 populations and geographic-climatic gradients (see e. g. De Kort et al., 2020; Galanti et al., 2022;
77 Lamka et al., 2022; Richards et al., 2017; Richards et al., 2010). In particular, global DNA
78 methylation tends to be lower in woody plants than perennial herbs, as well as in genomes of
79 widespread species compared to species with restricted geographic distributions (Alonso et al.,
80 2019a). Relevance of such life history traits when controlling for phylogenetic relatedness
81 remains largely unexplored and, thus, studies focused on analyzing natural variation in DNA
82 methylation of related species with contrasting ecological features should be particularly valuable
83 to better understand epigenomic similarities and divergences within and across plant species
84 (Medrano et al., 2020 and references therein; Noshay & Springer, 2021). Reduced representation
85 bisulfite DNA sequencing (RRBS) allows characterization of DNA methylation from a reduced
86 portion of the genome and can be applied to species even when no reference genome is available,
87 as it is usually the case for plants with narrow distribution ranges (Paun et al., 2019). Despite
88 limitations, RRBS can provide quantitative methylation information at the different sequence
89 contexts (CpG, CHG, CHH), together with an estimate of methylation similarity across
90 individuals and differentiation between populations and species, and may lead to some functional

91 characterization of methylated regions when an annotated reference genome of close relatives
92 and/or complementary RNAseq data is available (Chen et al., 2015; Hsu et al., 2017; Kreutz et
93 al., 2020; Nunn et al., 2021; Paun et al., 2019).

94 In this study, we explore the DNA methylation variation in natural plant populations of two
95 *Erodium* species co-occurring in Cazorla mountain ranges (South East Spain): the endemic woody
96 perennial *E. cazorlanum*, and the widespread annual herb *E. cicutarium*. Given the differences in
97 habitat specialization, distribution range and life history of these two congeneric species, we
98 predict they could differ in their genome-wide DNA methylation level and in the way epigenetic
99 variation is structured within and among populations throughout a geographical area where both
100 species co-exist. In particular, we predict that (1) individuals of the endemic *E. cazorlanum* will
101 exhibit higher diversity in genomic methylation levels than genetic variants, and (2) that
102 epigenetic variability should be less structured in space in the endemic species compared to its
103 widespread congener given the expected reduced range in suitable environmental conditions for
104 the former. To address so, we generated Restriction site-Associated DNA sequencing (RADseq)
105 data, both untreated and treated with bisulfite (bsRADseq, Trucchi et al., 2016), from leaf DNA
106 of the two *Erodium* species, each collected from three different localities. First, we checked for
107 population genetic structure in each species using the single nucleotide polymorphisms (SNPs)
108 obtained from RADseq data. We then estimated the percentage of DNA methylation per cytosine
109 in the three methylation contexts to search for quantitative and qualitative differences in genome-
110 wide DNA methylation at the species and locality levels using the bsRADseq data. Next, we
111 identified differentially methylated cytosines (DMCs), used them to estimate population
112 epigenetic structure in each species, and summarized them in differentially methylated regions
113 (DMRs) to characterize genomic loci potentially under divergent epigenetic regulation, at locality
114 and species level. Challenges derived from using a single incomplete reference genome to analyze
115 both species are discussed at the end.

2. Materials and methods

2.1. Study species and sample collection

Erodium cazorlanum (Heywood) is an endemic, long-lived woody perennial plant, typically associated to a few dolomite outcrops in Sierra de Cazorla-Segura-Las Villas Natural Park (Jaén, SE Spain) (Alonso & García-Sevilla, 2013). *Erodium cicutarium* (L.) L'Hér. is a widespread, herbaceous annual plant species with a fast life-cycle, frequently associated with ruderal habitats, and to more developed soils within the same study area (Fiz-Palacios *et al.,* 2010). The genome size of *E. cicutarium* has been estimated to range from 1.2 to 2.7 Gbps (Pustahija et al., 2013; Zonneveld, 2019), different ploidy levels have been reported from different geographic regions, ranging from diploid to tetraploid (Pustahija et al., 2013; Zonneveld, 2019), and preliminary data suggest our plants have 2n = 40 chromosomes. Genomic information about *E. cazorlanum* is scarce, but its estimated genome size is 8.1 Gbps (Alonso *et al.* unpublished data), it is described as an octoploid (Alonso & García-Sevilla, 2013; Blanca et al., 2009) and preliminary data suggest our plants have 2n = 80 chromosomes.

Young fully-developed leaves from 18 *E. cazorlanum* and 18 *E. cicutarium* individuals were collected at flowering within three localities per species in Sierra de Cazorla-Segura-Las Villas Natural Park (Jaén, Spain, **Figure 1**). The number of individuals per locality was selected based on available information on minimum sample sizes required for accurate estimates of intra- and inter-population genetic diversity based on high-throughput DNA sequencing (Nazareno et al., 2017). The study localities (hereafter populations) were Fuente Bermejo (FB), Puerto Lézar (PL), and Puerto del Tejo (PT) for *E. cazorlanum*; and Nava Correhuelas (CH), Fuente Bermejo (FB), and Puerto del Tejo (PT) for *E. cicutarium*. Horizontal distances between the nearest and farthest sampling sites were 7.5 and 19.4 km for *E. cazorlanum* (FB-PL and PL-PT, respectively), and 2.1 and 11.5 km for *E. cicutarium* (CH-FB and FB-PT, respectively). Note that despite sharing some sampling localities, the two species were located in separated patches due to differences in soil requirements (Moreno, 2008). Sampling details are thoroughly described in (Medrano et al., 2020).

143 **2.2. DNA extraction, library preparation, sequencing and quality check**

144 Total genomic DNA was extracted using Bioline ISOLATE II Plant DNA Kit and quantified
145 using a Qubit fluorometer 2.0 (Thermo Fisher Scientific, Waltham, MA, USA). The RADseq
146 library preparation followed the general steps from (Balao et al., 2023) (see **Supplementary**
147 **Materials & Methods** for details). Half the DNA yield per sample was treated with bisulfite to
148 generate bsRADseq libraries (Trucchi et al., 2016), the other half remained untreated for
149 generating RADseq libraries.

150 Both untreated and bisulfite-treated DNA samples were sequenced at the VBCF Vienna
151 (https://www.viennabiocenter.org/vbcf/next-generation-sequencing/) as paired-end 2 x 150 bp
152 reads, a single lane of an Illumina HiSeq 2500 machine was used for the untreated samples of the
153 two species (RADseq) and another lane was used for the bisulfite-treated samples (bsRADseq).
154 Reads are accessible through the sequence read archive (SRA) from NCBI, under BioProject ID
155 PRJNA1071520. The reads were demultiplexed with deML (Renaud et al., 2015), and then
156 STACKS v2.41 (Rochette & Catchen, 2017), discarding reads with low quality scores according
157 to default parameters. Demultiplexed reads were trimmed and cleansed from Illumina adapter
158 sequences with Trimmomatic v0.39 (Bolger et al., 2014) using the options '*TrimmomaticPE -*
159 *phred33 ILLUMINACLIP:adapterList:2:30:10 LEADING:28 TRAILING:28*
160 *SLIDINGWINDOW:4:15 MINLEN:30*'.

161 **2.3. Population genetics analysis**

162 A draft genome of *E. cicutarium* based on PacBio single-molecule long-read sequencing and
163 Illumina short-reads sequencing was assembled and annotated (see **Supplementary Materials &**
164 **Methods** for the details). The draft genome v2 is available at NCBI Genome, under accession
165 JATABU000000000; PacBio reads are available at NCBI SRA, under BioProject ID
166 PRJNA984161. Trimmed reads from the RADseq libraries were aligned to the *E. cicutarium* draft
167 genome v2 using *bowtie2* v2.2.5 (Langmead & Salzberg, 2012) with the '*--very-sensitive*' option.
168 Mapped reads were analyzed with the STACKS script *ref_map.pl*, and then single nucleotide

169 polymorphisms (SNPs) were filtered using STACKS binary *populations* with options '*-r 0.83 --*
170 *min_maf 0.05 --max_obs_het 0.7 --vcf --write_single_snp*'. For each species separately,
171 remaining SNPs were analyzed with PLINK v1.90b7 (Purcell et al., 2007) to perform Principal
172 Component Analysis (PCA) to summarize the genomic variation. Further, each SNP dataset was
173 analyzed with ADMIXTURE v1.3.0 (Alexander & Lange, 2011) to test the population genetic
174 structure of each species, testing for K values from 1 to 6, choosing the best fit for the K value
175 with the lowest cross-validation error. Pairwise genetic distance matrices between individuals
176 within a species were generated from the SNP dataset using the *distance* function of PLINK, that
177 calculates pairwise identity-by-state (IBS) distances based on allele counts from alleles shared for
178 each pairwise comparison. As an alternative approach, additional analyses for SNP calling and
179 population structure were performed with different model assumptions as implemented in the
180 genotype likelihood-based methods of *ANGSD* (Korneliussen et al., 2014) and *NGSadmix* (Skotte
181 et al., 2013) (see **Supplementary Materials & Methods** for details). Despite being developed
182 for diploid organisms, ANGSD was suggested as a powerful approach to disentangle genetic
183 patterns in heteroploid datasets (Zaveska et al., 2019). Naturally occurring C/T polymorphic sites
184 found in any of the two RADseq dataset were masked in the *E. cicutarium* genome for
185 downstream analyses.

186 **2.4. Alignment of bisulfite converted reads to genome**

187 Trimmed reads from the bsRADseq were aligned to the same *E. cicutarium* draft genome using
188 *bismark* v0.23.1 (Krueger & Andrews, 2011), with *Bowtie2* as base aligner (Langmead &
189 Salzberg, 2012), using the following options: *'--bowtie2 --non_directional --*
190 *most_valid_alignments 2 --L 32 --D 10 --R 1 --score_min L,0,0.2'*. For each individual, we
191 checked the summary report recording the mapping efficiency, the number of cytosines screened,
192 and the distribution among the different contexts (CpG, CHG, and CHH). The next step was to
193 extract the methylation information of each cytosine position using
194 *bismark_methylation_extractor*, with the options *'--no_overlap --ignore 4 --report --bedGraph -*
195 *-counts --CX'*. As in each read pair, the read corresponding to the sonicated end incorporates an

196 unmethylated cytosine in its first position during library construction, which then is exposed to
197 bisulfite treatment, bisulfite conversion rate (BCR) was calculated for each sample using the
198 formula $100 * T / (T + C)$, where T and C are the respective percentage of thymines and cytosines
199 in the first position of the 2nd paired read (Krueger, 2013).

200 **2.5. Global DNA methylation analysis**

201 Unless otherwise stated, all statistical analyses were performed using R v4.1.2 (R Core Team,
202 2023). The number of methylated cytosines and total number of genomic positions analyzed per
203 individual was extracted from *bismark* reports with a custom R script. Global effects associated
204 to species and population divergence on global genome methylation levels were analyzed with a
205 GLM with quasibinomial distribution and logit link, using *emmeans* (Lenth, 2023) and *lme4*
206 (Bates et al., 2015) R packages. The dependent variable was the overall proportion of methylated
207 to unmethylated cytosines per individual, and the formula included species as fixed factor and
208 populations of each separate species as a nested fixed factor (formula: proportion of methylated
209 cytosines ~ species + species : population). The same process was done for each methylation
210 context separately (CpG, CHG, CHH).

211 **2.6. Differential methylation analysis**

212 Detection of differentially methylated cytosines (DMCs) between populations was conducted
213 with *DSS* v2.46.0 R package (Feng et al., 2014; Park & Wu, 2016). *DSS* is based on a beta-
214 binomial regression model with arcsine link function, and it takes advantage of shrinkage
215 estimation of the dispersion parameter based on a Bayesian hierarchical model to reduce the
216 dependence of variance on mean. P-values were adjusted for multiple testing using the Benjamini
217 and Hochberg false discovery rate (FDR) procedure, retaining those with FDR < 0.05 (Benjamini
218 & Hochberg, 1995). Analyses were conducted for each species separately. Although *DSS* allowed
219 fitting a model with a single factor with three populations as levels, handling RRBS data reduces
220 the probability of finding single cytosine positions well covered for all three populations (i.e., a
221 position showing acceptable coverage for two populations, but not covered in the remaining

222 population), which would discard potential DMCs due to insufficient coverage. Thus, differences
223 in cytosine methylation between pairs of populations were calculated fitting the data to one-factor
224 models consisting in pairs of populations, generating six datasets (FB x PL, FB x PT and PL x PT
225 for *E. cazorlanum*; CH x FB, CH x PT and FB x PT for *E. cicutarium*). A position was considered
226 a DMC when its FDR between populations was < 0.05, and the difference in methylation was >
227 20 % between any of the paired-population comparisons. This approach implies that the definition
228 of hyper- and hypo-methylation is relative: a single DMC can be considered as hyper-methylated
229 in one or more populations, and at the same time hypo-methylated in other population(s). Number
230 of overlapping DMCs (either hyper- or hypo-methylated DMCs) from two populations were
231 analyzed with a hypergeometric test to investigate whether overlaps were greater than expected
232 by chance.

233 Hierarchical clustering and visualization based on methylation percentage per DMC was
234 calculated and plotted using *pheatmap* R package (Kolde 2019). The variation observed in
235 percentage of methylation across DMCs was also analyzed with non-metric multidimensional
236 scaling (NMDS) in *vegan* R package (Oksanen et al., 2022), with 100 random starting
237 configurations and choosing the Manhattan distance method. Sets of DMCs which showed 100
238 % methylation in a single individual and methylation percentages close to zero in the rest of the
239 individuals were named "drastic" DMCs, the rest of DMCs were named "gradual" DMCs.
240 Hierarchical clustering and NMDS analyses were performed again with only "gradual" DMCs.

241 Epigenetic Euclidean distance matrices between individuals within a species were calculated from
242 the methylation percentage matrix of gradual DMCs using *vegan* R package (Oksanen et al.,
243 2022). The complete DMC set and only "gradual" DMC set epigenetic matrices were compared
244 with previously calculated genetic distance matrices with a Mantel test, to test for intra-specific
245 Spearman correlation between genetic and epigenetic distance, with 9,999 permutations, using
246 *vegan* R package. Additional Mantel's tests to check the relationship between genetic and
247 epigenetic distances were also performed on each separated methylation context (CpG, CHG and
248 CHH).

249 Differentially methylated regions (DMRs) between populations were detected using *callDMRs()*
250 function from the *DSS* package with default parameters. Methylation site density (MSD) per
251 DMR was calculated by dividing the number of DMCs found in the DMR by the total length in
252 base pairs of the respective DMR. After observing the MSD frequency distribution, percentile 90
253 of each population comparison's MSD distribution was calculated and used as threshold to filter
254 potential false positive DMRs (i. e. long DMRs with a relatively small number of DMCs). A DMR
255 was retained when three or more DMCs were present within a genomic region with a minimum
256 length of 50 bps and when its MSD value was higher than the percentile 90 of the MSD
257 distribution for the analyzed comparison. After considering the biological differences of CpG,
258 CHG and CHH methylation contexts, we opted to call DMRs as groups of DMCs from the same
259 methylation context (CpG, CHG and CHH).

260 **2.7. Inter-species comparison**

261 The mean percentage of uniquely mapped bsRADseq reads to *E. cicutarium* draft reference
262 genome was 19.00 % [13.6 % - 25.6 %] for *E. cazorlanum* samples, and 58.40 % [47.2 % - 72.6
263 %] for *E. cicutarium* samples (**Supplementary Table S1**), which showed statistically significant
264 differences (ANOVA F statistic = 515.91, df = 1, P-value < 0.001). Given the different mapping
265 rates, biases in differential methylation analysis were expected when cytosine and methylated
266 cytosine coverages were compared between species. Thus, a normalization factor was applied to
267 *E. cicutarium* read counts before comparing methylation levels between species. The
268 normalization factor was calculated as the mean mapping efficiency from *E. cazorlanum* samples
269 divided by the mean mapping efficiency for *E. cicutarium*, and *E. cicutarium* read counts were
270 normalized by multiplying both the coverage and methylated cytosines counts per locus by the
271 obtained normalization factor. Raw read counts in *E. cazorlanum* and normalized read counts in
272 *E. cicutarium* were used for DMC and DMR calling analyses in the interspecies comparison.
273 Priors for considering a DMC and a DMR were the same as the ones explained in previous
274 sections above.

275 **2.8. Functional characterization of differentially methylated regions**

276 DMCs included in DMRs that overlapped either with exons, introns, 5' UTRs, 3' UTRs or
277 intergenic regions as described in the *E. cicutarium* draft genome were identified with custom
278 scripts. DMCs that overlapped with repeated elements from the *E. cicutarium* genome, including
279 transposable elements (TEs), were retrieved with the *CNEr* R package (Tan et al., 2019). Fisher's
280 exact test was used to test whether the proportion of TEs overlapping with the *E. cicutarium* set
281 of DMCs/DMRs was over- or under-represented compared to the proportion of all the TEs present
282 in the *E. cicutarium* draft genome.

283 GO terms were extracted from the gene annotation file of the *E. cicutarium* draft genome with a
284 custom script. Lists of DMRs overlapping with annotated genes were then analyzed with *topGO*
285 (Alexa & Rahnenfuhrer, 2023) to find enriched GO terms in each DMR list, using a weighted
286 Fisher's exact test and correcting the p-value with FDR. A GO term was considered
287 enriched/over-represented in a set when the FDR < 0.05.

288 **3. Results**

289 **3.1. Sequencing quality and bisulfite treatment efficiency.**

290 For the 36 samples, Illumina sequencing produced a total of 332.2 million 2 x 150 bp length
291 paired-end reads for RADseq (ranging from 3.4 to 12.2 million per sample in *E. cazorlanum*, and
292 from 4.4 to 33.8 million per sample in *E. cicutarium*), and a total of 323.4 million 2 x 150 bp
293 length paired-end reads for bsRADseq (ranging from 3 to 13.6 million per sample in *E.*
294 *cazorlanum*, and from 3.8 to 30 million per sample in *E. cicutarium*). After removing adapters
295 and checking the distribution of sequencing quality per nucleotide, 315.3 million reads were
296 retained in the RADseq, and 302.4 million reads remained in the bsRADseq. Mean bisulfite
297 conversion rate per sample was 99.09 % [99.07 % - 99.13 %] (**Supplementary Table S1**).

298 **3.2. Genetic polymorphism and population structure**

299 A total of 24,977 SNPs in *E. cazorlanum* and 31,696 SNPs in *E. cicutarium* passed the filtering
300 process. In the endemic *E. cazorlanum*, the PCA shows clustering by sampling locality mainly on
301 PC1, but the position of the groups did not follow a geographical pattern, with some individuals
302 from different localities positioned very close together in the multidimensional PCA. Individuals
303 from the FB population appeared more clearly separated from the other two populations, although
304 all principal components explained less than 10 % of the variance on their own (**Figure 1**).
305 ADMIXTURE considered *E. cazorlanum* as a single genetic entity (K = 1) based on minimizing
306 the cross-validation error, whereas higher numbers of potential populations did not differentiate
307 between the different localities. For the widespread *E. cicutarium*, the PCA shows three separated
308 groups: one with all the individuals from CH and FB populations, another with four individuals
309 from PT population, and the third one with two individuals from PT population (**Figure 1**); the
310 difference between the first two groups is supported by PC1 (20.3 % of explained variance) and
311 the difference between the first and third group is described by PC2 (13.5 % of explained
312 variance). ADMIXTURE again considered *E. cicutarium* individuals as a single genetic entity (K
313 = 1) based on the cross validation error (**Supplementary Figure S1**). **Figure 1** shows assignment

314 of *E. cazorlanum* and *E. cicutarium* individuals to subpopulations, assuming models with two to
315 six subpopulations. **Supplementary Table S2** shows the cross-validation error values.
316 Alternative analyses performed with the genotype likelihood-based method of *ANGSD* showed
317 consistent results with the ones shown above (see **Supplementary Materials & Methods** for
318 details).

319 **3.3. Global DNA methylation analysis.**

320 *Bismark* analyzed a total of 11,921,613 cytosines in any methylation context (1.49 % of *E.*
321 *cicutarium* draft genome total length). Percentages of global DNA methylation ranged from 6.66
322 % to 12.71 % in the endemic *E. cazorlanum* and from 7.76 % to 11.07 % in the widespread *E.*
323 *cicutarium* (**Supplementary Table S1**). Within species variance of global methylation
324 percentages was higher for *E. cazorlanum* (**Table 1**). **Figure 2** shows the methylated cytosine
325 percentages per sequence context by species and by population. On average, there were significant
326 differences between the two species in the ratio of methylated to unmethylated cytosines per
327 individual (**Table 2**) with the genomes of *E. cazorlanum* being more methylated (mean ± SD =
328 9.51 ± 1.83) compared to *E. cicutarium* (mean ± SD = 9.08 ± 0.94). Similar results were also
329 obtained for each of the three methylation contexts (**Table 2**, **Supplementary Figure S2**).
330 Differences in percentages of global DNA methylation were also statistically significant between
331 the study populations within a species, as were all pairwise within-species population contrasts
332 (**Table 2**, **Supplementary Figure S2**). Further, within species variance was always higher for *E.*
333 *cazorlanum* global and context specific methylation percentages (**Table 1**).

334 **3.4. Differential cytosine methylation analysis within species.**

335 A total of 12,795 and 16,131 naturally occurring C/T polymorphic sites obtained from RADseq
336 analyses were masked in bsRADseq data before analyses in *E. cazorlanum* (0.11 % of analyzed
337 Cs) and *E. cicutarium* (0.14 % of analyzed Cs), respectively. For *E. cazorlanum*, a total of 13,643
338 DMCs (5,632 CpG, 2,605 CHG, 5,406 CHH) were detected between the three populations (ca.
339 0.11 % of total analyzed Cs), and 47,615 DMCs (ca. 0.40 % of total analyzed Cs) were detected

340 between the three populations of *E. cicutarium* (20,670 CpG, 8,278 CHG, 18,667 CHH;
341 **Supplementary Figure S3**, **Supplementary Tables S3, S4, S5**). In each of the two species, the
342 number of overlapping hyper- or hypo-methylated DMCs between each population pair was never
343 significantly greater than expected by chance (hypergeometric test, P-value = 1, **Supplementary**
344 **Figures S4, S5**). The overlap of DMCs between species was also not greater than predicted by
345 chance either (hypergeometric test, P-value = 1, **Supplementary Figure S6**).

346 Hierarchical clustering of DMCs showed that most clusters were defined by cytosines with
347 "drastic" changes in methylation percentage within the study dataset (i. e., 100 % methylation for
348 one individual and ca. 0 % methylation for the rest, **Supplementary Figure S7**). Removing these
349 "drastic" DMCs and leaving only those with "gradual" change in methylation percentage still did
350 not group samples following a clear population structure in any of the two species (**Figure 3,**
351 **Supplementary Figure S7**). When analyzing the "gradual" DMCs by separated methylation
352 context, the CpG context DMCs showed clusters with at least three samples from the same
353 population for *E. cazorlanum*, and more patently for *E. cicutarium*; while CHG and CHH contexts
354 did not group more than three samples from the same population within any cluster
355 (**Supplementary Figures S8, S9**).

356 Multivariate analysis based on all DMCs showed no clear population segregation in *E.*
357 *cazorlanum* and a slight differentiation of the PT population for *E. cicutarium* (**Figure 3**). The
358 same analysis, but performed only with gradual DMCs, marginally increased the differentiation
359 of PT population from FB and CH in *E. cicutarium*, while not affecting *E. cazorlanum* grouping
360 pattern (**Figure 3**). Performing multivariate analyses with DMCs separated by context did not
361 improve segregation of populations (**Supplementary Figures S10, S11**).

362 Mantel tests revealed no statistically significant correlation between pairwise genetic and
363 epigenetic distances across individuals in any of the two study species (*E. cazorlanum*: Mantel's
364 R = 0.104, p-value = 0.271; *E. cicutarium*: Mantel's R = 0.003, p-value = 0.471). When
365 considering epigenetic distances exclusively for each separate methylation context, Mantel tests
366 also showed no statistical significance (p-value > 0.05).

367 **3.5. Genomic and functional characterization of DMRs.**

368 Only DMRs with high density of DMCs (defined as DMRs above the percentile 90 of the MSD
369 distribution; **Supplementary Figure S12, Supplementary Table S6**) were selected for further
370 characterization. **Supplementary Table S7** shows the full list of DMRs that passed the filter,
371 including a total of 43 DMRs defined between populations of the endemic *E. cazorlanum* that
372 vary in length between 53 and 165 bp, and 145 DMRs defined between populations of the
373 widespread *E. cicutarium* that vary in length between 51 and 343 bp. GO term enrichment analysis
374 did not reveal enriched GO terms in any set of DMRs. In *E. cazorlanum*, we found 19 DMRs
375 whose available annotation was associated with genes involved in plant development, amino acid
376 metabolism, or stress response. In *E. cicutarium*, 49 out of 145 DMRs showed available
377 annotation, and were associated with plant development, stress response, signaling, and cell wall
378 homeostasis, among other biological processes.

379 The two species showed an overall similar pattern regarding DMR overlapping with genomic
380 features (**Figure 4**). DMRs in CpG context (17 in *E. cazorlanum*, 18 in *E. cicutarium*) overlapped
381 most frequently with exons in both species (93.8 % in *E. cazorlanum*, 61.1 % in *E. cicutarium*),
382 while DMRs in CHH context (24 in *E. cazorlanum*, 125 in *E. cicutarium*) overlapped evenly with
383 exons, introns and intergenic regions. The number of DMRs in CHG context (three in *E.*
384 *cazorlanum*, two in *E. cicutarium*, all overlapping with exons) is too low to reach any clear
385 conclusion. Altogether, from the 43 DMRs found in *E. cazorlanum*, 29 (67.4 %) overlapped with
386 exons, six (14.0 %) did so with introns, four (9.3 %) with intergenic regions, two overlapped
387 simultaneously with an exon and an intron (4.7 %), one with a 5'UTR (2.3 %), and one (2.3 %)
388 with a 3' UTR. We found more evenly distributed overlaps in the 145 DMRs found between
389 populations of *E. cicutarium*: 44 (30.6 %) overlapped with intergenic regions, 42 (29.2 %) with
390 exons, 41 (28.5 %) with introns, eleven with an exon and an intron (7.6 %), four (2.8 %) with a
391 3'UTR, one with an intron and a 3'UTR (0.7 %) and one with a 5'UTR and an exon (0.7 %). A
392 higher proportion of DMRs was found in intergenic regions in *E. cicutarium* (30.56 %) compared
393 to *E. cazorlanum* (9.30 %).

394 Regarding DMRs overlapping with transposable elements (TEs), most of them occurred in DMRs
395 associated to CHH methylation context: 14 out of 15 DMRs overlapping with TEs involved
396 methylation changes in CHH in *E. cazorlanum* (93.33 %), and all the 26 DMRs overlapping with
397 TEs in *E. cicutarium* involved only methylation changes in CHH (**Figure 4**). In *E. cazorlanum*,
398 TEs with most overlaps with DMRs were LTRs (with eleven *Copia* and two *Gypsy* elements
399 overlapping with a DMR), followed by three DNA TEs (one *MULE-MuDR*, one *CMC-EnSpm*,
400 and one uncharacterized DNA element overlapping with a DMR). For *E. cicutarium*, the most
401 overlapped TE family was also *Copia* with 13 DMRs, in addition, it showed six *LINE/L1*, three
402 *PIF-Harbingers*, one *MULE-MuDR*, one *hAT-Tag1*, one *CMC-EnSpm*, and one *Gypsy* element
403 overlapping with DMRs. **Supplementary Table S8** shows all overlaps between a DMR with a
404 genome feature, a TE, or both.

405 The set of DMRs from *E. cicutarium* showed a higher than expected proportion of overlaps with
406 *Copia* TEs compared with the proportion of *Copia* TEs in the genome of *E. cicutarium* (χ^2 =
407 3.522, df = 1, p-value = 0.045, **Supplementary Figure S13, Supplementary Table S9**). An
408 analogous analysis in *E. cazorlanum* was not conducted because the TE set in *E. cazorlanum*
409 genome may be substantially different from *E. cicutarium* genome, making the comparison
410 between *E. cazorlanum* TEs in DMRs and *E. cicutarium* TE genome set inadequate.

411 **3.6. Comparative analysis between species.**

412 Given the difference in read mapping efficiency between species (**Supplementary Figure 14**),
413 we used the ratio between mean mapping efficiencies (0.33) as normalization factor when
414 comparing *E. cicutarium* read coverage values with *E. cazorlanum*. First, we compared samples
415 from *E. cazorlanum* and *E. cicutarium* before normalization of *E. cicutarium* read counts,
416 detecting 10,765 DMCs (2,790 CpG, 2,272 CHG, 5,703 CHH) and 113 DMRs (12 CpG, 24 CHG,
417 77 CHH). After normalization, we found 13,744 DMCs (6,739 CpG, 2,154 CHG, 4,851 CHH,
418 **Supplementary Table S10, Supplementary Figure S14**) and 183 DMRs (109 CpG, 23 CHG,
419 51 CHH), which were reduced to 19 DMR (5 CpG, 2 CHG, 12 CHH) after filtering by MSD
420 (**Supplementary Table S11, Supplementary Figures S14, S15**). Similarity in the number of

421 DMCs before and after normalization was significantly greater than expected for all contexts
422 (hypergeometric test, P-value < 0.001), although the direction of the loss of DMCs was not the
423 same for the three sequence contexts: 3,961, 232, and 351 DMCs were gained, while 12, 350 and
424 1,203 DMCs were lost after normalization in CpG, CHG and CHH contexts, respectively. Before
425 and after normalization, *E. cicutarium* showed more hyper-methylated CpG sites compared to *E.*
426 *cazorlanum*, while *E. cazorlanum* showed more hyper-methylation in CHG and CHH contexts
427 compared to *E. cicutarium*.

428 Hierarchical clustering based on methylation percentage of the DMCs did not show a perfect
429 divergence of species, but clades showed a species-like pattern rather than a population-like
430 pattern, and the use of "gradual" DMCs did not change this pattern (**Supplementary Figure S16**).
431 Multivariate analyses revealed a separation between centroids of the two species, a higher
432 dispersion in *E. cicutarium* samples, and little within-species population variation, either using
433 all DMCs or "gradual" DMCs (**Supplementary Figure S17**).

434 Among the 19 inter-specific DMRs obtained, we found association with an endochitinase
435 (hydrolyses chitin and chitodextrins), *Cytohesin-2* (involved in regulation of protein sorting and
436 membrane trafficking) and *pre-mRNA-splicing factor CEF1* (involved in cell cycle control)
437 hyper-methylated in the CHH context in *E. cazorlanum*. The only DMR hyper-methylated in *E.*
438 *cicutarium* was associated to the *LTL1* gene (involved in salt tolerance mechanisms) with
439 increased methylation in the CpG context. Eleven DMRs from the inter-species comparison
440 overlapped with exons, five with introns, two with an intergenic region, one with a 3' UTR, and
441 another one with both an exon and an intron. Ten DMRs from the inter-species comparison
442 overlapped with fourteen TEs. They were mostly unknown repeats (eight out of 14), but also
443 included three *Copia*, one *Gypsy*, one *SINE/tRNA-V*, and one *PIF-Harbinger* elements
444 (**Supplementary Table S12**).

445 **4. Discussion**

446 This study analyzes variation in both DNA sequence (genetic) and cytosine methylation levels
447 (epigenetic) at single-base resolution in natural populations of two *Erodium* species, the endemic
448 *E. cazorlanum* and the widespread *E. cicutarium*, using bsRADseq and the structural and
449 functional annotation provided by a draft reference genome developed *ad hoc* for the study
450 species with the smallest genome (*E. cicutarium*). The two species exhibited sound differences in
451 life history (woody perennial *vs*. annual), habitat specialization (dolomite specialist *vs*. ruderal)
452 and geographic distribution range (local narrow endemic *vs*. world-wide widespread) that allowed
453 us to test the hypothesis that population genetic and epigenetic structure within the region of
454 coexistence would differ according to each species ecological features, with stronger epigenetic
455 than genetic population structure in the least specialized (*E. cicutarium*). Besides, the use of
456 methods that provide accurate genomic information of the methylation markers allowed the
457 identification of a set of candidate genes whose epigenetic regulation might vary across the study
458 localities of each species according to the recorded differences in DNA methylation, paving the
459 avenue towards more specific analysis of adaptive strategies in species with contrasting genomic
460 and ecological features. In the following paragraphs, we will first discuss the limitations of the
461 reduced representation methodology used when applied to species with contrasting genome
462 features and resources (see also Paun et al., 2019). Then, we will discuss the results obtained for
463 our study system and how they reinforce the *a priori* prediction mentioned above.

464 **4.1. Challenges and opportunities of RRBS analyses in plant ecological epigenetics**

465 In absence of any high-quality gapless genome for any species in the *Erodium* genus, RRBS was
466 the best available option to simultaneously detect natural genome and methylome variants across
467 populations and explore their genomic location. In retrospective, six samples per population were
468 estimated sufficient to reach an appropriate level of representation of what occurs in wild plant
469 populations in genomics studies (Nazareno et al., 2017), and by using RRBS we expected to
470 generate informative methylation datasets when conjointly used with genomic data for the same

471 individuals (Gawehns et al., 2022; Paun et al., 2019). In fact, several studies have successfully
472 identified differentially methylated loci by optimizing RRBS and its downstream analysis in
473 commercial plant species with available reference genome (e.g., *Brassica rapa,* Chen et al., 2015;
474 maize, Hsu et al., 2017). In this study, we succeeded in obtaining differentially methylated
475 cytosines (DMC) and regions (DMR) between populations in the two *Erodium* species with six
476 individuals per population, despite the limited power for differential methylation analysis
477 presumed for the afforded sample sizes (Lea et al., 2017).

478 Interpretation of the results obtained for the portion of genome here explored should take into
479 account that due to the relatively high GC content in the recognition site of the specific enzyme
480 we used (*Pst*I that cuts at CTGCAG), bsRADseq dataset is enriched for genic regions (Lea et al.,
481 2017; Trucchi et al., 2016) and, thus, quantitative global estimates would be less accurate for
482 genomes with a relative high content of repetitive elements (i.e., in *E. cazorlanum* according to
483 its larger genome size). Nevertheless, percentages of cytosine methylation per sequence context
484 in the two species were consistent among each other and also with those reported for other plant
485 species with complete methylomes, i.e., CpG higher than CHG, CHH being the lowest (Cokus et
486 al., 2008; De Kort et al., 2020; Hsu et al., 2017; Zhao et al., 2020). The higher proportion of
487 methylated to unmethylated cytosines obtained in *E. cazorlanum* is consistent with a marked
488 difference in percentages obtained from independent analyses conducted by HPLC to obtain
489 global DNA methylation estimates for the two species (28.4 % *vs*. 18.2 %; Alonso unpublished
490 data). The sign of divergence in estimates of global DNA methylation per species could be
491 associated to the largest genome size of *E. cazorlanum* (Alonso et al., 2015; Vidalis et al., 2016).
492 The higher heterogeneity in overall methylation estimates of study individuals obtained for *E.*
493 *cazorlanum* could be due to either genome size, and some unmeasured micro-environmental
494 features (Valverde et al., 2024) or a combination of the two effects.

495 Further, using the reference genome from a close relative species generated a homology bias
496 during the alignment of the reads that may weaken the potential for functional annotation of loci
497 with divergent methylation in *E. cazorlanum*. Accordingly, the few DMRs obtained in *E.*

498 *cazorlanum* were located in exonic regions, likely due to a higher similarity in the coding regions
499 of the two species' genomes and not necessarily to absence of methylation divergence in genomic
500 regions that were not captured (Lea et al., 2017).

501 Altogether, our study exemplifies the challenges of applying NGS markers to species with limited
502 genomic resources and complex genomes. However, conducting epigenomic studies of such
503 species is compulsory to improve our current understanding of ecological factors behind the huge
504 variation in global DNA methylation across plant species, that require a broad phylogenetic
505 perspective (Alonso et al., 2015), and might be useful to better characterize the sources of
506 variation in DNA methylation at plant ecosystem or community levels (Alonso et al., 2019b;
507 Boquete et al., 2021). Our results support the use of RRBS for interspecific comparisons of natural
508 variation in DNA methylation at difference sequence contexts, and a more restricted power to
509 explore candidate genes and transposable elements potentially differentially regulated by DNA
510 methylation when high-quality reference genomes are not available (Paun et al., 2019).

511 **4.2. Genetic and methylation variation in natural populations of *E. cazorlanum* and *E.***
512 ***cicutarium***

513 In the small geographic area here explored, selected populations of each of the two study species
514 lack or show limited signs of genetic population structure, suggesting they are well connected to
515 each other, showing most genetic variation between individuals from the same population.
516 Whereas this fact should be taken with caution for extrapolation to broader geographic areas, all
517 study individuals could be associated to a single genetic background eventually, making the
518 investigation of methylation variants more straightforward. Spontaneous epimutations, i.e.
519 random changes in methylation status of cytosines, are estimated to be four to five orders of
520 magnitude higher than mutation rate in *Arabidopsis*, which may facilitate the decoupling of
521 methylation variation from genetic variation and some specific contribution to heritable
522 phenotypic variation (Banta & Richards, 2018; Denkena et al., 2021; van der Graaf et al., 2015;
523 Weng et al., 2019). In this study, we found absence of correlation between genetic and epigenetic

524 distances across individuals in the two study species, supporting it would be worth to
525 experimentally exploring their relative contribution to individual phenotypes and their plasticities
526 under controlled environmental conditions (see e.g. Williams et al., 2023).

527 **4.3. Genomic characterization of DNA methylation variants and functional annotation of**
528 **DMRs**

529 In each of the two species, most methylation changes between individuals with different
530 population of origin were found in CpG and CHH contexts compared to a much lower frequency
531 in CHG. A high level of CHH methylation variation is expected given the sensitivity of this
532 context to environmental changes (Dubin et al., 2015); in fact, there is evidence that epigenetic
533 distance based in CHH methylation differences can be positively correlated with climatic distance
534 in *Thlaspi arvense* (Galanti et al., 2022). In the endemic *E. cazorlanum*, natural variation in
535 methylation at those DMCs did not exhibit any population structure, regardless the analyses
536 considered all or context-specific DMCs. In the widespread *E. cicutarium*, we found some
537 epigenetic differentiation between the three study populations, supporting our expectation that, in
538 absence of genetic population structure, the broader habitat conditions expected in a widespread
539 species could contribute to larger methylation variance between study individuals at different
540 scales (Valverde et al., 2024).

541 We only proceed with functional annotation of DMRs because solid experimental evidence has
542 linked methylation gains and losses in large genomic regions (i.e., DMRs) with transcriptional
543 variation and heritable phenotypic effects, whereas the functional relevance of single methylation
544 changes (i.e., DMCs) might be more variable across plant species (De Kort et al., 2022; Denkena
545 et al., 2021). Furthermore, although our analytical procedure based on *Bismark* concentrates
546 exclusively on uniquely mapping reads that in turn will result in a depletion of representation of
547 repetitive genomic elements, there was also a fair number of DMRs overlapping with TEs in our
548 *E. cicutarium* data. As a rule, methylation levels in TEs are maintained high in plants to silence
549 their expression and maintain genome stability (Matzke & Mosher, 2014). In our TE annotated

550 bsRADseq data, the *Copia* family was the most abundant, and it was found overlapping with
551 DMRs in a higher than expected proportion compared to the total number of TEs identified in the
552 *E. cicutarium* draft genome. The expression of *Copia* TE family seems stress responsive in several
553 plant species (Ito et al., 2011, 2016; Klein & Anderson, 2022), suggesting that *Copia* elements
554 with CHH methylation islands in promoter regions that have shifted methylation between our
555 study locations might be potentially linked to stress genes' expression regulation. Additional
556 studies in *E. cicutarium*, in which changes in DNA methylation caused by 5-azacytidine and the
557 effect of recurrent drought were experimentally addressed, also found that induced DMRs were
558 enriched with *Copia* elements (Balao et al., 2023), supporting the idea that this TE family may
559 have a stress-related regulatory function in *E. cicutarium* too.

560 Finally, deep differences in read coverage obtained for the two species could cause biases in the
561 direct inter-specific comparison of methylation landscapes offered by DMC detection. Following
562 a normalization step to equilibrate coverage inspired in library size normalization for RNA-seq
563 data (Conesa et al., 2016; Zeng & Mortazavi, 2012), we found that the overall number of detected
564 DMCs between the two species was practically the same, although the relative frequency per
565 sequence context changed and more significant methylation changes in CpG were retained after
566 normalization. Further studies comparing two or more related species with a single available
567 reference genome would be required to validate this methodology. Interestingly, main differences
568 in genomic methylation profiles observed by DMC detection between the two study species
569 involved hypermethylation in non-CpG sites in *E. cazorlanum* and hypomethylation of CpG sites,
570 except when included in DMRs that were most frequently hypermethylated in all contexts.

571 **4.4. Conclusions and future steps.**

572 With limited genomic resources typically available for non-model plants of conservation concern,
573 this study compared DNA methylation at single-base resolution in a reduced portion of the
574 genomes of two congeneric species and explored their spatial structure in a small area of
575 coexistence. We found support for (i) an overall higher global DNA methylation in the endemic
576 *E. cazorlanum*, particularly associated to hypermethylation in non-CpG sites, and in agreement

with its higher genome size compared to its widespread congener *E. cicutarium*. (ii) The absence of genetic population structure in the endemic species, and (iii) the lack of correlation between genetic and epigenetic variation across individuals of both species, suggest that they could have independent effects on individual phenotypes. Finally, (iv) a slightly higher DNA methylation divergence between study populations in *E. cicutarium* supports the hypothesis that a stronger epigenetic, rather than genetic, population structure could be expected in widespread generalist species (see also Valverde et al. 2024). Future studies should take the advantage of the genomic resources generated here to link phenotypic, genetic and epigenetic variation in experimental settings suitable to identify the epigenetic contribution to plant adaptation to environmental variation.

Author contributions

CA obtained funding for the study. MM, FB, OP, CA designed the experimental setting. MM and CA conducted fieldwork, PB performed molecular lab work. RM-B analyzed the data. RM-B wrote the first draft of the paper, with feedback from FB, OP and CA. All co-authors provided comments and suggestions on the final version of the manuscript and approved it.

Acknowledgements

The authors gratefully thank to Noelia Zarza for assisting us during field sampling; to Ben Zonneveld (Netherlands) for determining the genomic sizes of *E. cazorlanum* and *E. cicutarium*; to Abelardo Aparicio (University of Sevilla, Spain) for determining the ploidy levels of *E. cazorlanum* and *E. cicutarium*; and to Carlos M. Herrera, Javier Valverde, Javier Puy and Anupoma N. Troyee (Estación Biológica de Doñana, Spain) for providing valuable discussion. Funding for this work has been provided by grant EPIENDEM (CGL2016-76605-P) from the Spanish Ministero de Economía y Competitividad, and grants EPINTER (PID2019-104365GB-I00) and DISTEPIC (PID2022-141530NB-C22) from the Spanish Ministerio de Ciencia e Innovación.

602 **Data accessibility and Benefit-generation statement**

603 Illumina raw sequence reads are deposited in the SRA (BioProject PRJNA1071520). PacBio long
604 reads are also deposited in the SRA (BioProject PRJNA984161). Draft genome assembly is
605 deposited in NCBI Genome repository (accession JATABU000000000). Scripts are available
606 under personal request to RM-B and CA. Benefits Generated: Benefits from this research accrue
607 from the sharing of our data and results on public databases as described above.

608 **ORCID**

609 Rubén Martín-Blázquez: https://orcid.org/0000-0002-4400-6514

610 Mónica Medrano: https://orcid.org/0000-0002-2816-4192

611 Pilar Bazaga: https://orcid.org/0000-0002-8295-4937

612 Francisco Balao: https://orcid.org/0000-0003-2104-3846

613 Ovidiu Paun: https://orcid.org/0000-0002-8295-4937

614 Conchita Alonso: https://orcid.org/0000-0002-7418-3204

615 **References**

616 Alexa, B., & Rahnenfuhrer, J. (2023). topGO: Enrichment Analysis for Gene Ontology. Retrieved
617 from https://bioconductor.org/packages/topGO doi:10.18129/B9.bioc.topGO

618 Alexander, D. H., & Lange, K. (2011). Enhancements to the ADMIXTURE algorithm for
619 individual ancestry estimation. *BMC Bioinformatics,* **12**, 246. doi: 10.1186/1471-2105-
620 12-246

621 Alonso, C., & García-Sevilla, M. (2013). Strong inbreeding depression and individually variable
622 mating system in the narrow endemic *Erodium cazorlanum* (Geraniaceae). *Anales del*
623 *Jardín Botánico de Madrid,* **70**(1), 72-80. doi:10.3989/ajbm

624 Alonso, C., Medrano, M., Perez, R., Canto, A., Parra-Tabla, V., & Herrera, C. M. (2019a).
625 Interspecific variation across angiosperms in global DNA methylation: phylogeny,
626 ecology and plant features in tropical and Mediterranean communities. *New Phytologist,*
627 **224**(2), 949-960. doi:10.1111/nph.16046
628 Alonso, C., Perez, R., Bazaga, P., & Herrera, C. M. (2015). Global DNA cytosine methylation as
629 an evolving trait: phylogenetic signal and correlated evolution with genome size in
630 angiosperms. *Frontiers in Genetics,* **6**, 4. doi:10.3389/fgene.2015.00004
631 Alonso, C., Ramos-Cruz, D., & Becker, C. (2019b). The role of plant epigenetics in biotic
632 interactions. *New Phytologist,* **221**(2), 731-737. doi:10.1111/nph.15408
633 Anderson, J. T., & Gezon, Z. J. (2015). Plasticity in functional traits in the context of climate
634 change: a case study of the subalpine forb *Boechera stricta* (Brassicaceae). *Global*
635 *Change Biology l,* **21**(4), 1689-1703. doi:10.1111/gcb.12770
636 Balao, F., Medrano, M., Bazaga, P., Paun, O., & Alonso, C. (2023). Long-term methylome
637 changes after experimental seed demethylation and their interaction with recurrent water
638 stress in *Erodium cicutarium* (Geraniaceae). *bioRxiv*. doi:10.1101/2023.01.19.524693
639 Balao, F., Paun, O., & Alonso, C. (2018). Uncovering the contribution of epigenetics to plant
640 phenotypic variation in Mediterranean ecosystems. *Plant Biology ,* **20** (S1), 38-49.
641 doi:10.1111/plb.12594
642 Banta, J. A., & Richards, C. L. (2018). Quantitative epigenetics and evolution. *Heredity ,* **121**(3),
643 210-224. doi:10.1038/s41437-018-0114-x
644 Bates, D., Mächler, M., Bolker, B., & Walker, S. (2015). Fitting linear mixed-effects models using
645 *lme4*. *Journal of Statistical Software,* **67**(1). doi:10.18637/jss.v067.i01
646 Benjamini, Y., & Hochberg, Y. (1995). Controlling the false discovery rate: a practical and
647 powerful approach to multiple testing. *Journal of the Royal Statistical Society: series B*
648 *(Methodological),* **57**(1), 289-300. doi:10.1111/j.2517-6161.1995.tb02031.x
649 Bewick, A. J., & Schmitz, R. J. (2017). Gene body DNA methylation in plants. *Current Opinion*
650 *in Plant Biology,* **36**, 103-110. doi:10.1016/j.pbi.2016.12.007

651 Blanca, G., Cabezudo, B., Cueto, M., Fernández López, C., & Morales Torres, C. (2009). *Flora*
652 *Vascular de Andalucía Oriental. Volumen 3: Rosaceae–Lentibulariaceae*: Consejería de
653 Medio Ambiente, Junta de Andalucía, Sevilla.
654 Bolger, A. M., Lohse, M., & Usadel, B. (2014). Trimmomatic: a flexible trimmer for Illumina
655 sequence data. *Bioinformatics,* **30**(15), 2114-2120. doi:10.1093/bioinformatics/btu170
656 Boquete, M. T., Muyle, A., & Alonso, C. (2021). Plant epigenetics: phenotypic and functional
657 diversity beyond the DNA sequence. *American Journal of Botany,* **108**(4), 553-558.
658 doi:10.1002/ajb2.1645
659 Bossdorf, O., Richards, C. L., & Pigliucci, M. (2008). Epigenetics for ecologists. *Ecology Letters,*
660 **11**(2), 106-115. doi:10.1111/j.1461-0248.2007.01130.x
661 Bouyer, D., Kramdi, A., Kassam, M., Heese, M., Schnittger, A., Roudier, F., & Colot, V. (2017).
662 DNA methylation dynamics during early plant life. *Genome Biology,* **18**(1), 179.
663 doi:10.1186/s13059-017-1313-0
664 Chen, X., Ge, X., Wang, J., Tan, C., King, G. J., & Liu, K. (2015). Genome-wide DNA
665 methylation profiling by modified reduced representation bisulfite sequencing in
666 *Brassica rapa* suggests that epigenetic modifications play a key role in polyploid genome
667 evolution. *Frontiers in Plant Science,* **6**, 836. doi:10.3389/fpls.2015.00836
668 Cokus, S. J., Feng, S., Zhang, X., Chen, Z., Merriman, B., Haudenschild, C. D., Pradhan, S.,
669 Nelson, S. F., & Pellegrini, M., & Jacobsen, S. E. (2008). Shotgun bisulphite sequencing
670 of the *Arabidopsis* genome reveals DNA methylation patterning. *Nature,* **452**(7184), 215-
671 219. doi:10.1038/nature06745
672 Conesa, A., Madrigal, P., Tarazona, S., Gomez-Cabrero, D., Cervera, A., McPherson, A.,
673 Szcześniak, M. W., Gaffney, D. J., Elo, L. L., Zhang, X., & Mortazavi, A. (2016). A
674 survey of best practices for RNA-seq data analysis. *Genome Biology,* **17**, 13.
675 doi:10.1186/s13059-016-0881-8
676 De Kort, H., Panis, B., Deforce, D., Van Nieuwerburgh, F., & Honnay, O. (2020). Ecological
677 divergence of wild strawberry DNA methylation patterns at distinct spatial scales.
678 *Molecular Ecology,* **29**(24), 4871-4881. doi:10.1111/mec.15689

679 De Kort, H., Toivainen, T., Van Nieuwerburgh, F., Andres, J., Hytonen, T. P., & Honnay, O.
680 (2022). Signatures of polygenic adaptation align with genome-wide methylation patterns
681 in wild strawberry plants. *New Phytologist,* **235**(4), 1501-1514. doi:10.1111/nph.18225
682 Denkena, J., Johannes, F., & Colome-Tatche, M. (2021). Region-level epimutation rates in
683 *Arabidopsis thaliana*. *Heredity,* **127**(2), 190-202. doi:10.1038/s41437-021-00441-w
684 Du, J., Zhong, X., Bernatavichute, Y. V., Stroud, H., Feng, S., Caro, E., Vashisht, A. A., Terragni,
685 J., Chin, H. G., Tu, A., Hetzel, J., Wohlschlegel, J. A., Pradhan, S., Patel, D.J., &
686 Jacobsen, S. E. (2012). Dual binding of chromomethylase domains to H3K9me2-
687 containing nucleosomes directs DNA methylation in plants. *Cell,* **151**(1), 167-180.
688 doi:10.1016/j.cell.2012.07.034
689 Dubin, M. J., Zhang, P., Meng, D., Remigereau, M. S., Osborne, E. J., Paolo Casale, F., Drewe,
690 P., Kahles, A., Jean, G., Vilhjálmsson, B., Jagoda, J., Irez, S., Voronin, V., Song, Q.,
691 Long, Q., Rätsch, G., ,Stegle, O., Clark, R. M., & Nordborg, M. (2015). DNA methylation
692 in *Arabidopsis* has a genetic basis and shows evidence of local adaptation. *eLife,* **4**,
693 e05255. doi:10.7554/eLife.05255
694 Feng, H., Conneely, K. N., & Wu, H. (2014). A Bayesian hierarchical model to detect
695 differentially methylated loci from single nucleotide resolution sequencing data. *Nucleic*
696 *Acids Research,* **42**(8), e69. doi:10.1093/nar/gku154
697 Fiz-Palacios, O., Vargas, P., Vila, R., Papadopulos, A. S., & Aldasoro, J. J. (2010). The uneven
698 phylogeny and biogeography of *Erodium* (Geraniaceae): radiations in the Mediterranean
699 and recent recurrent intercontinental colonization. *Annals of Botany* **106**: 871-884.
700 doi:10.1093/aob/mcq184
701 Galanti, D., Ramos-Cruz, D., Nunn, A., Rodríguez-Arevalo, I., Scheepens, J. F., Becker, C., &
702 Bossdorf, O. (2022). Genetic and environmental drivers of large-scale epigenetic
703 variation in *Thlaspi arvense*. *PLoS Genetics,* **18**(10), e1010452.
704 doi:10.1371/journal.pgen.1010452

705 Gawehns, F., Postuma, M., van Antro, M., Nunn, A., Sepers, B., Fatma, S., van Gurp, T. P.,
706 Wagemaker, N. C. A. M., Mateman, A. C., Milanovic-Ivanovic, S., Groβe, I., van Oers,
707 K., Vergeer, P., & Verhoeven, K. J. F. (2022). epiGBS2: Improvements and evaluation
708 of highly multiplexed, epiGBS-based reduced representation bisulfite sequencing.
709 *Molecular Ecology Resources,* **22**(5), 2087-2104. doi:10.1111/1755-0998.13597
710 Hawes, N. A., Fidler, A. E., Tremblay, L. A., Pochon, X., Dunphy, B. J., & Smith, K. F. (2018).
711 Understanding the role of DNA methylation in successful biological invasions: a review.
712 *Biological Invasions,* **20**(9), 2285-2300. doi:10.1007/s10530-018-1703-6
713 Herrera, C. M., Alonso, C., Medrano, M., Perez, R., & Bazaga, P. (2018). Transgenerational
714 epigenetics: Inheritance of global cytosine methylation and methylation-related
715 epigenetic markers in the shrub *Lavandula latifolia*. *American Journal of Botany,* **105**(4),
716 741-748. doi:10.1002/ajb2.1074
717 Herrera, C. M., Medrano, M., Bazaga, P., & Alonso, C. (2022). Ecological significance of
718 intraplant variation: Epigenetic mosaicism in *Lavandula latifolia* plants predicts extant
719 and transgenerational variability of fecundity-related traits. *Journal of Ecology,* **110**(11),
720 2555-2567. doi:10.1111/1365-2745.13964
721 Hsu, F. M., Yen, M. R., Wang, C. T., Lin, C. Y., Wang, C. R., & Chen, P. Y. (2017). Optimized
722 reduced representation bisulfite sequencing reveals tissue-specific mCHH islands in
723 maize. *Epigenetics Chromatin,* **10**(1), 42. doi:10.1186/s13072-017-0148-y
724 Ito, H., Gaubert, H., Bucher, E., Mirouze, M., Vaillant, I., & Paszkowski, J. (2011). An siRNA
725 pathway prevents transgenerational retrotransposition in plants subjected to stress.
726 *Nature,* **472**(7341), 115-119. doi:10.1038/nature09861
727 Ito, H., Kim, J. M., Matsunaga, W., Saze, H., Matsui, A., Endo, T. A., Harukawa Y., Takagi H.,
728 Yaegashi H., Masuta Y., Masuda S., Ishida J., Tanaka M., Takahashi S., Morosawa T.,
729 Toyoda T., Kakutani T., Kato A., & Seki, M. (2016). A stress-activated transposon in
730 *Arabidopsis* induces transgenerational abscisic acid insensitivity. *Scientific Reports,* **6**,
731 23181. doi:10.1038/srep23181

732 Kidwell, M. G. (2002). Transposable elements and the evolution of genome size in eukaryotes.
733 *Genetica,* **115**, 49-63. doi:10.1023/a:1016072014259.
734 Klein, S. P., & Anderson, S. N. (2022). The evolution and function of transposons in epigenetic
735 regulation in response to the environment. *Current Opinion in Plant Biology,* **69**, 102277.
736 doi:10.1016/j.pbi.2022.102277
737 Kolde, R. (2019). pheatmap: pretty heatmaps. R package version 1.0.12. Retrieved from
738 https://CRAN.R-project.org/package=pheatmap
739 Korneliussen, T. S., Albrechtsen, A., & Nielsen, R. (2014). ANGSD: Analysis of Next Generation
740 Sequencing Data. *BMC Bioinformatics,* **15**(356). doi:10.1186/s12859-014-0356-4
741 Kreutz, C., Can, N. S., Bruening, R. S., Meyberg, R., Merai, Z., Fernandez-Pozo, N., & Rensing,
742 S. A. (2020). A blind and independent benchmark study for detecting differeally
743 methylated regions in plants. *Bioinformatics,* **36**(11), 3314-3321.
744 doi:10.1093/bioinformatics/btaa191
745 Krueger, F. (2013). Reduced Representation Bisulfite-Seq – A Brief Guide to RRBS. Retrieved
746 from https://www.bioinformatics.babraham.ac.uk/projects/bismark/RRBS_Guide.pdf
747 Krueger, F., & Andrews, S. R. (2011). Bismark: a flexible aligner and methylation caller for
748 Bisulfite-Seq applications. *Bioinformatics,* **27**(11), 1571-1572.
749 doi:10.1093/bioinformatics/btr167
750 Lamka, G. F., Harder, A. M., Sundaram, M., Schwartz, T. S., Christie, M. R., DeWoody, J. A., &
751 Willoughby, J. R. (2022). Epigenetics in ecology, evolution, and conservation. *Frontiers*
752 *in Ecology and Evolution,* **10**, 871791. doi:10.3389/fevo.2022.871791
753 Langmead, B., & Salzberg, S. L. (2012). Fast gapped-read alignment with Bowtie 2. *Nature*
754 *Methods,* **9**(4), 357-359. doi:10.1038/nmeth.1923
755 Law, J. A., & Jacobsen, S. E. (2010). Establishing, maintaining and modifying DNA methylation
756 patterns in plants and animals. *Nature Reviews Genetics,* **11**(3), 204-220.
757 doi:10.1038/nrg2719

758 Lea, A. J., Vilgalys, T. P., Durst, P. A. P., & Tung, J. (2017). Maximizing ecological and
759 evolutionary insight in bisulfite sequencing data sets. *Nature Ecology & Evolution,* **1**(8),
760 1074-1083. doi:10.1038/s41559-017-0229-0
761 Lenth, R. (2023). emmeans: Estimated marginal means, aka least-squares means. Retrieved from
762 https://CRAN.R-project.org/package=emmeans
763 Matzke, M. A., & Mosher, R. A. (2014). RNA-directed DNA methylation: an epigenetic pathway
764 of increasing complexity. *Nature Reviews Genetics,* **15**(6), 394-408.
765 doi:10.1038/nrg3683
766 Medrano, M., Alonso, C., Bazaga, P., López, E., & Herrera, C. M. (2020). Comparative genetic
767 and epigenetic diversity in pairs of sympatric, closely related plants with contrasting
768 distribution ranges in south-eastern Iberian mountains. *AoB Plants,* **12**(3), plaa013.
769 doi:10.1093/aobpla/plaa013
770 Moreno, J. C. (2008). *Lista Roja 2008 de la Flora Vascular Española*: Ministerio de Medio
771 Ambiente y Medio Rural y Marino.
772 Muyle, A. M., Seymour, D. K., Lv, Y., Huettel, B., & Gaut, B. S. (2022). Gene body methylation
773 in plants: Mechanisms, functions, and important implications for understanding
774 evolutionary processes. *Genome Biology and Evolution,* **14**(4). doi:10.1093/gbe/evac038
775 Nazareno, A. G., Bemmels, J. B., Dick, C. W., & Lohmann, L. G. (2017). Minimum sample sizes
776 for population genomics: an empirical study from an Amazonian plant species. *Molecular*
777 *Ecology Resources,* **17**(6), 1136-1147. doi:10.1111/1755-0998.12654
778 Noshay, J. M., & Springer, N. M. (2021). Stories that can't be told by SNPs; DNA methylation
779 variation in plant populations. *Current Opinion in Plant Biology,* **61**, 101989.
780 doi:10.1016/j.pbi.2020.101989
781 Nunn, A., Can, S. N., Otto, C., Fasold, M., Díez Rodríguez, B., Fernández-Pozo, N., Rensing, S.
782 A., Stadler, P. F., & Langenberger, D. (2021). EpiDiverse Toolkit: a pipeline suite for the
783 analysis of bisulfite sequencing data in ecological plant epigenetics. *NAR Genomomics*
784 *Bioinformatics,* **3**(4), lqab106. doi:10.1093/nargab/lqab106

785 Oksanen, J., Simpson, G. L., Blanchet, F. G., Kindt, R., Legendre, P., Minchin, P. R., O'Hara, R.
786 B., Simpson, G. L., Solymos, P., Stevens, M., Szoecs, E., Wagner, H., Barbour, M.,
787 Bedward, M., Bolker, B., Borcard, D., Carvalho, G., Chirico, M., De Caceres, M.,
788 Durand, S., & Weedon, J. (2022). Vegan: Community ecology package. R package
789 version 2.6-2. Retrieved from https://CRAN.R-project.org/package=vegan
790 Park, Y., & Wu, H. (2016). Differential methylation analysis for BS-seq data under general
791 experimental design. *Bioinformatics,* **32**(10), 1446-1453.
792 doi:10.1093/bioinformatics/btw026
793 Paun, O., Verhoeven, K. J. F., & Richards, C. L. (2019). Opportunities and limitations of reduced
794 representation bisulfite sequencing in plant ecological epigenomics. *New Phytologist,*
795 **221**(2), 738-742. doi:10.1111/nph.15388
796 Purcell, S., Neale, B., Todd-Brown, K., Thomas, L., Ferreira, M. A., Bender, D., Maller, J., Sklar,
797 P., De Bakker, P. I., Daly, M. J., & Sham, P. C. (2007). PLINK: a tool set for whole-
798 genome association and population-based linkage analyses. *American Journal of Human*
799 *Genetics,* **81**(3), 559-575. doi:10.1086/519795
800 Pustahija, F., Brown, S. C., Bogunić, F., Bašić, N., Muratović, E., Ollier, S., Hidalgo, O., Bourge,
801 M., Stevanović, V., & Siljak-Yakovlev, S. (2013). Small genomes dominate in plants
802 growing on serpentine soils in West Balkans, an exhaustive study of 8 habitats covering
803 308 taxa. *Plant and Soil,* **373**(1-2), 427-453. doi:10.1007/s11104-013-1794-x
804 R Core Team (2023). R: A language and environment for statistical computing. R Foundation for
805 Statistical Computing.
806 Renaud, G., Stenzel, U., Maricic, T., Wiebe, V., & Kelso, J. (2015). deML: robust demultiplexing
807 of Illumina sequences using a likelihood-based approach. *Bioinformatics,* **31**(5), 770-772.
808 doi:10.1093/bioinformatics/btu719
809 Richards, C. L., Alonso, C., Becker, C., Bossdorf, O., Bucher, E., Colomé-Tatché, M., Durka,
810 W., Engelhardt, J., Gaspar, B., Gogol-Döring, A., Grosse, I., van Gurp, T. P., Heer, K.,
811 Kronholm, I., Lampei, C., Latzel, V., Mirouze, M., Opgenoorth, L., Paun, O., &
812 Verhoeven, K. J. F. (2017). Ecological plant epigenetics: Evidence from model and non-

model species, and the way forward. *Ecology Letters,* **20**(12), 1576-1590. doi:10.1111/ele.12858

Richards, C. L., Bossdorf, O., & Verhoeven, K. J. F. (2010). Understanding natural epigenetic variation. *New Phytologist,* **187**(3), 562-564.

Richards, E. J. (2006). Inherited epigenetic variation —revisiting soft inheritance. *Nature Reviews,* **7**, 395-401.

Rochette, N. C., & Catchen, J. M. (2017). Deriving genotypes from RAD-seq short-read data using Stacks. *Nature Protocols,* **12(**12), 2640-2659. doi:10.1038/nprot.2017.123

Schmitz, R. J., Schultz, M. D., Lewsey, M. G., O'Malley, R. C., Urich, M. A., Libiger, O., Schork, N. J., & Ecker, J. R. (2011). Transgenerational epigenetic instability is a source of novel methylation variants. *Science,* **334**, 369-373. doi: 10.1126/science.1212959

Skotte, L., Korneliussen, T. S., & Albrechtsen, A. (2013). Estimating individual admixture proportions from next generation sequencing data. *Genetics,* **195**(3), 693-702. doi:10.1534/genetics.113.154138

Stroud, H., Do, T., Du, J., Zhong, X., Feng, S., Johnson, L., Patel, D. J., & Jacobsen, S. E. (2014). Non-CG methylation patterns shape the epigenetic landscape in *Arabidopsis*. *Nature Structural and Molecular Biology,* **21**(1), 64-72. doi:10.1038/nsmb.2735

Szukala, A., Bertel, C., Frajman, B., Schonswetter, P., & Paun, O. (2023). Parallel adaptation to lower altitudes is associated with enhanced plasticity in *Heliosperma pusillum* (Caryophyllaceae). *The Plant Journal,* **115**(6), 1619-1632. doi:10.1111/tpj.16342

Tan, G., Polychronopoulos, D., & Lenhard, B. (2019). CNEr: a toolkit for exploring extreme noncoding conservation. *PLoS Computational Biology,* **15**(8), e1006940.

Trucchi, E., Mazzarella, A. B., Gilfillan, G. D., Lorenzo, M. T., Schonswetter, P., & Paun, O. (2016). BsRADseq: screening DNA methylation in natural populations of non-model species. *Molecular Ecology,* **25**(8), 1697-1713. doi:10.1111/mec.13550

Valverde, J., Medrano, M., Herrera, C. M., & Alonso, C. (2024). Comparative epigenetic and genetic spatial structure in Mediterranean mountain plants: a multispecies study. *Heredity,* **132**(2), 106-116. doi:10.1038/s41437-024-00668-3

841 van der Graaf, A., Wardenaar, R., Neumann, D. A., Taudt, A., Shaw, R. G., Jansen, R. C.,
842 Schmitz, R. J., Colomé-Tatché, M., & Johannes, F. (2015). Rate, spectrum, and
843 evolutionary dynamics of spontaneous epimutations. *Proceedings of the National*
844 *Academy of Sciences of the United States of America,* **112**(21), 6676-6681.
845 doi:10.1073/pnas.1424254112
846 Varotto, S., Krugman, T., Aiese Cigliano, R., Kashkush, K., Kondic-Spika, A., Aravanopoulos,
847 F. A., Pradillo, M., Consiglio, F., Aversano, R., Pecinka, A., & Miladinovic, D. (2022).
848 Exploitation of epigenetic variation of crop wild relatives for crop improvement and
849 agrobiodiversity preservation. *Theoretical and Applied Genetics,* **135**(11), 3987-4003.
850 doi:10.1007/s00122-022-04122-y
851 Vidalis, A., Zivkovic, D., Wardenaar, R., Roquis, D., Tellier, A., & Johannes, F. (2016).
852 Methylome evolution in plants. *Genome Biology,* **17**(1), 264. doi:10.1186/s13059-016-
853 1127-5
854 Weng, M. L., Becker, C., Hildebrandt, J., Neumann, M., Rutter, M. T., Shaw, R. G., Weigel, D.,
855 & Fenster, C. B. (2019). Fine-grained analysis of spontaneous mutation spectrum and
856 frequency in *Arabidopsis thaliana*. *Genetics,* **211**(2), 703-714.
857 doi:10.1534/genetics.118.301721
858 Williams, B. R., Miller, A. J., & Edwards, C. E. (2023). How do threatened plant species with
859 low genetic diversity respond to environmental stress? Insights from comparative
860 conservation epigenomics and phenotypic plasticity. *Molecular Ecology Resources*.
861 doi:10.1111/1755-0998.13897
862 Záveská, E., Maylandt, C., Paun, O., Bertel, C., Frajman, B., The STEPPE Consortium, &
863 Schönswetter, P. (2019). Multiple auto- and allopolyploidisations marked the Pleistocene
864 history of the widespread Eurasian steppe plant *Astragalus onobrychis* (Fabaceae).
865 *Molecular Phylogenetics and Evolution*, **139**. doi:10.1016/j.ympev.2019.106572
866 Zeng, W., & Mortazavi, A. (2012). Technical considerations for functional sequencing assays.
867 *Nature Immunology,* **13**(9), 802-807. doi:10.1038/ni.2407

868 Zhao, L., Xie, L., Zhang, Q., Ouyang, W., Deng, L., Guan, P., Ma, M., Li, Y., Zhang, Y., Xiao,
869 Q., Zhang, J., Li, H., Wang, S., Man, J., Cao, Z., Zhang, Q., Zhang, Q., Li, G., & Li, X.
870 (2020). Integrative analysis of reference epigenomes in 20 rice varieties. *Nature*
871 *Communications,* **11**(1), 2658. doi:10.1038/s41467-020-16457-5
872 Zonneveld, B. J. M. (2019). The DNA weights per nucleus (genome size) of more than 2350
873 species of the Flora of The Netherlands, of which 1370 are new to science, including the
874 pattern of their DNA peaks. *Forum geobotanicum,* **8**, 24-78. doi:10.3264/FG.2019.1022

875

876

877 **Figures**

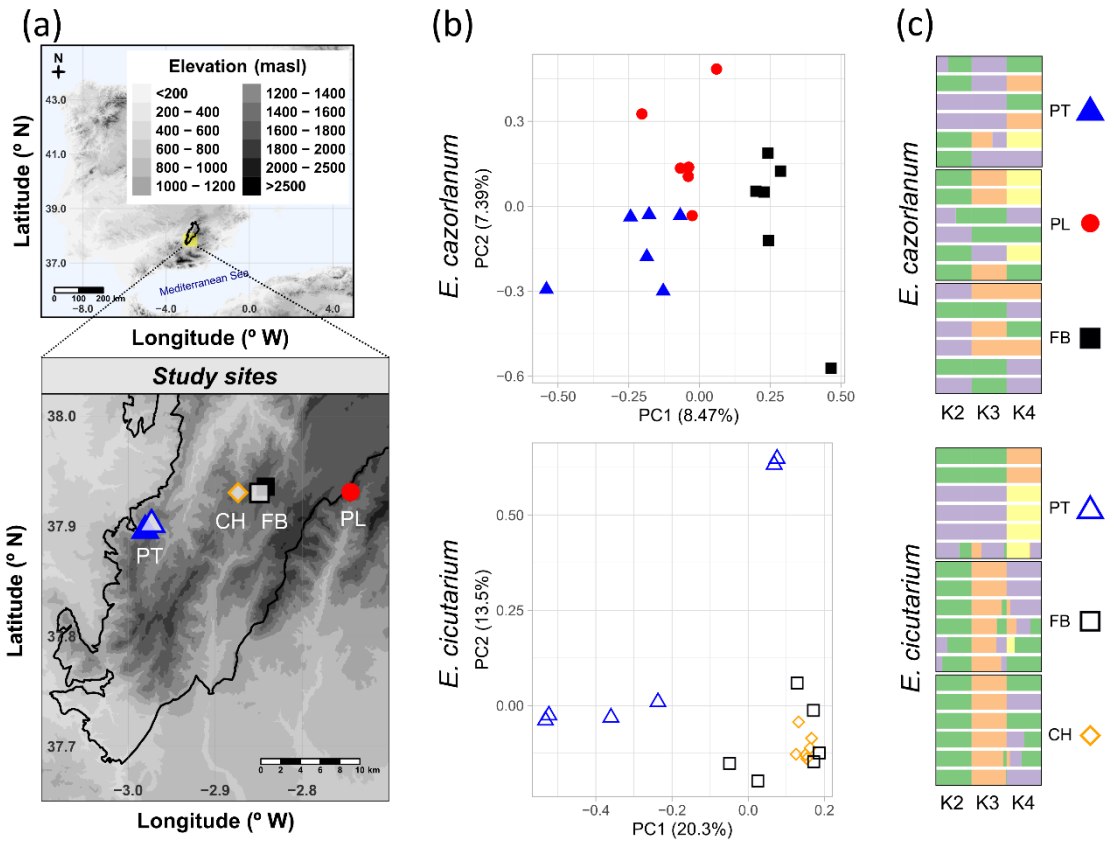

878

879 **Figure 1.** Genetic population structure of the two study species. A: Study area and localities. Top:
880 map of the Iberian Peninsula showing the area of the Parque Natural Sierras de Cazorla-Segura-
881 Las Villas (delimited by a solid black line) and the sampling area (yellow square). Altitude (masl
882 = meters above sea level) is represented as a grey scale. Bottom: Detail of the sampling area,
883 showing the study localities of *Erodium cazorlanum* and *E. cicutarium*. CH = Nava Correhuelas,
884 FB = Fuente Bermejo, PL = Puerto Lézar, PT= Puerto del Tejo. B: Principal component analysis
885 for *E. cazorlanum* (top) and *E. cicutarium* (bottom) based on SNPs obtained by RADseq. Each
886 biplot shows principal components PC1 and PC2 (together with their percentage of explained
887 variance) in X- and Y-axis, respectively; data points are individuals; populations are shown with
888 different colors and shapes. C: Admixture analysis for *E. cazorlanum* (top) and *E. cicutarium*
889 (bottom) based on SNPs from RADseq. X-axis shows the K value chosen for each model. Y-axis
890 shows all study individuals, with populations enclosed in different boxes. Colors represent

891 different modeled genetic lineages according to the selected K value. Each color within a tile
892 indicates the proportion of SNPs from different modeled lineages.

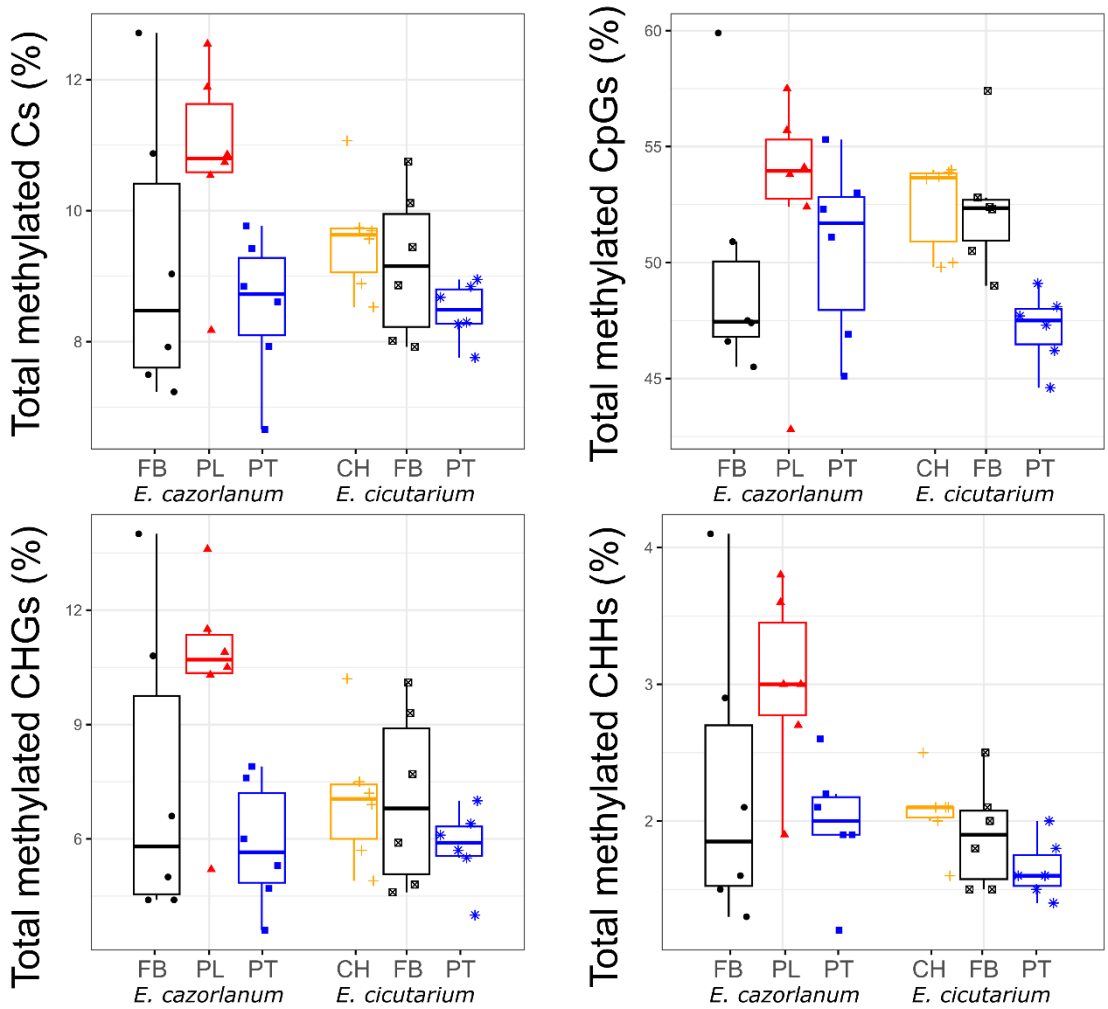

Figure 2. Variation in levels of DNA methylation in populations of *E. cazorlanum* and *E. cicutarium*. The plots show percent of all the sequenced cytosines that were methylated (top left) and estimates obtained for cytosines in the three methylation contexts: CpG (top right), CHG (bottom left) and CHH (bottom right). On each graph, symbols represent individuals, X-axis shows the study populations of the two *Erodium* species, and Y-axis shows the methylation percentage estimated. Each box shows the median (central line), quartiles 1 and 3 (bottom and top edges of the box), and maximum and minimum values (box whiskers) per population (represented by different colors and shapes). Note that Y-axes have different scales.

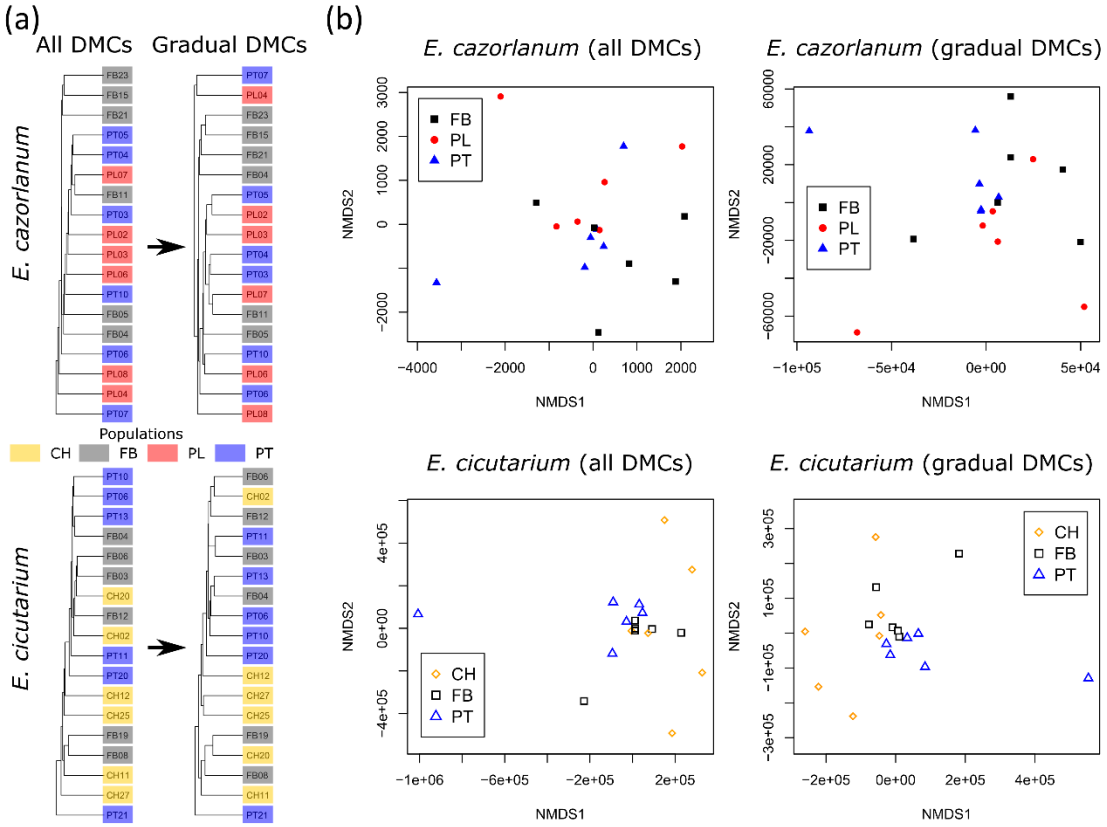

903

904 **Figure 3.** Epigenetic population structure of the two *Erodium* species. A: Hierarchical individual
905 clustering according to obtained differentially methylated cytosines (DMCs) based on percentage
906 of methylation per DMC locus. Top dendrograms correspond to *E. cazorlanum* (N = 13,643 loci)
907 and bottom dendrograms to *E. cicutarium* (N = 47,615 loci). Each column shows the resulting
908 clustering of all DMCs (left) and gradual DMCs (right), see text for details. Colored tiles attached
909 to each sample ID show the population of origin. B: Multilocus analysis of individual variation
910 in methylation percentage of all DMCs (left graphs) and gradual DMCs (right graphs) based on
911 non-metric multidimensional scaling (NMDS). Top graphs show data for *E. cazorlanum*, bottom
912 graphs for *E. cicutarium*. X and Y axes show non-linear multidimensional scaling (NMDS)
913 dimensions NMDS1 and NMDS2, respectively. Colors of data points show the population of
914 origin.

915

916

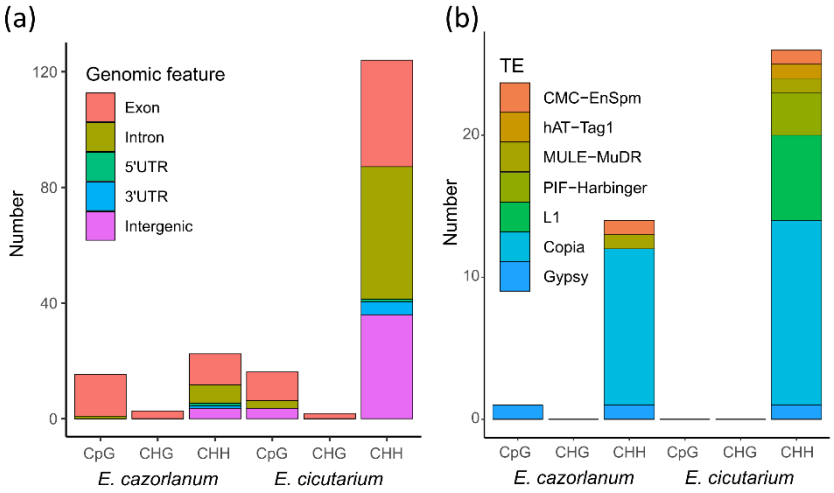

Figure 4. Genomic characterization of differentially methylated regions (DMRs) obtained for the two *Erodium* species. A: Genomic features overlapping with DMRs. X-axis shows the species and DMR methylation context (*E. cazorlanum*: CpG = 16, CHG = 3, CHH = 24; *E. cicutarium*: CpG = 18, CHG = 2, CHH = 125). Y-axis shows the numbers of DMRs found overlapping with each of the five different genomic features distinguished (exon, intron, 5'UTR, 3'UTR and intergenic regions). B: Transposable elements overlapping with DMRs. X-axis shows the species and DMR methylation context (*E. cazorlanum*: CpG = 1, CHG = 0, CHH = 14; *E. cicutarium*: CpG = 0, CHG = 0, CHH = 27). Y-axis shows the number of DMRs found overlapping with each of the nine families of TEs distinguished.

928 **Tables**

929 **Table 1.** Coefficients of variation of global DNA methylation percentages. First column shows
930 each methylation context. Each set of four columns shows information related to each species.
931 The first column of each species set shows CV from all populations, the three remaining
932 columns show CVs for each population.

933

	E. cazorlanum				*E. cicutarium*			
CVs	Overall	FB	PL	PT	Overall	CH	FB	PT
Total Cs	18.72%	22.54%	13.59%	12.54%	9.74%	7.55%	12.30%	5.41%
CpG	9.28%	10.77%	9.79%	7.65%	6.51%	3.85%	5.42%	3.34%
CHG	42.69%	52.90%	26.94%	28.58%	27.24%	25.79%	32.99%	17.68%
CHH	35.50%	47.68%	22.61%	23.31%	17.93%	13.91%	20.25%	13.14%

934

935

936 **Table 2.** Global cytosine methylation differences at species and population level. First column
937 shows the set of cytosines for which a binomial distribution model was run to test whether the
938 difference between the proportion of methylated to unmethylated cytosines (mC / uC) was
939 statistically significant. Columns two to four show log-ratio χ2, degrees of freedom, and p-value
940 for species. Columns five to seven show the same for populations within species.

	Species			Species:Population		
Proportion of mC / uC	LR χ^2	d.f.	P-value	LR χ^2	d.f.	P-value
Total Cs	74,280	1	< 0.001	918,941	4	< 0.001
CpG	2,118	1	< 0.001	627,781	4	< 0.001
CHG	146,988	1	< 0.001	498,203	4	< 0.001
CHH	340,129	1	< 0.001	426,370	4	< 0.001

941